Health Physics Vol. 55, No. 1 (July), pp. 15–29, 1988
Printed in the U.S.A.

0017-9078/88 $3.00 + .00
© 1988 Health Physics Society
Pergamon Press plc

● *Paper*

CALIBRATION FACTORS FOR Ge DETECTORS USED FOR FIELD SPECTROMETRY

Irene K. Helfer* and Kevin M. Miller**
Environmental Measurements Laboratory, U.S. Department of Energy, New York, NY 10014-3621

(*Received* 26 *June* 1987; *accepted* 17 *February* 1988)

***Abstract*—Calibration factors to convert a measured full-absorption peak count rate to activity in the soil and dose rate in air are given for Ge detectors that are used for field measurements of radionuclides. The appropriate factors for a given detector are derived using three primary parameters: the manufacturer's quoted efficiency at 1332 keV relative to a 7.6 cm (3 in.) long by 7.6 cm (3 in.) diameter NaI(Tl) detector, the detector's orientation in the field (up or down) and the Ge crystal length/diameter ratio. The accuracy of the results obtained by using this simplified calibration technique is estimated to be 10–15%.**

INTRODUCTION

AS A RESULT of the Three Mile Island incident in 1979, a need emerged for portable instrumentation that could be used for making rapid measurements in the field during emergency situations. Portable Ge detectors became available shortly thereafter and since have demonstrated their usefulness in the area of field spectrometry. These portable detectors have the same spectrometric capabilities as the standard large dewar types but are light weight and feature increased capabilities such as ruggedness, compactness and an all-attitude operation. With the advent of battery-powered portable microprocessor-based multichannel analyzers, a complete γ spectrometer system now can be hand carried by one person for use in remote areas.

Most γ spectrometrists are familiar with the laboratory calibration procedures used for fixed geometry sample analyses. However, for field work, they only may perform qualitative measurements by simply identifying the γ emitters present at a site. Semi-quantitative *in-situ* results are sometimes inferred by comparing peak count rates and obtaining a relative measure of contamination. Ideally, one would like to convert the count rate to some meaningful quantity such as dose rate or radionuclide concentration.

A Ge-γ spectrometer, whether portable or the standard large dewar-based type, has the capability to measure uncollided flux from various photon-emitting radionuclides in the environment. The Environmental Measurements Laboratory (EML) pioneered in studies involving the application of *in-situ* γ spectrometry (Beck et al. 1972) to many types of radiation studies. These applications include the measurement of residual ^{137}Cs levels in soils (Miller and Helfer 1985), an analysis of power plant reactor plumes (Gogolak 1984) and surveys of indoor exposure rates (Miller and Beck 1984). *In-situ* spectrometry proved to be extremely valuable in making rapid measurements of fission products in the environment during the Three Mile Island incident (Miller et al. 1979) and most recently was used with the same success by European laboratories during the Chernobyl crisis (Gogolak et al. 1986). In all of these applications, the measured photon flux can be converted into the inventory (activity per unit area) or concentration of a particular radionuclide in the soil and/or the exposure rate in the air based on a knowledge of the source distribution.

Since the adoption of Ge detectors for field spectrometry in 1971, EML has calibrated eight coaxial Ge detectors of various types and efficiencies. These were commercial units, purchased from two different manufacturers, that included Ge(Li) and high purity P-type and N-type Ge, ranging in efficiency from 3%–45% (at 1332 keV relative to a 7.6 cm [3 in.] long × 7.6 cm [3 in.] diameter NaI[Tl] detector). The calibration data for these detectors have been reevaluated and correlated to the detector crystal dimensions and manufacturer's quoted efficiency. Based on this information, we present here analytical functions and tabular data that can be used to provide reasonably accurate field calibration factors for others to apply to their own Ge detectors.

FIELD SETUP PROCEDURES

In order to obtain accurate measurements of radionuclides in the soil, the Ge detector should be placed on

* Present Address: Law Associates, 2 University Plaza Suite 201, Hackensack, NJ 07601.
** To whom correspondence should be addressed.

relatively even and open terrain. Areas where there are large obstructions such as boulders or man-made structures should be avoided. When working in wooded areas, the detector should be positioned away from tree trunks as far as possible. When measuring fallout radionuclides, the terrain under study also should be undisturbed since natural wind and water erosion processes as well as any human activity, such as plowing, would upset the distribution of any deposited radionuclides. Although these site criteria can be difficult to meet for aged fallout, there is generally no problem for a fresh deposition event: a typical large lawn would qualify. For measurements in most undisturbed terrain, one generally can assume a uniform distribution with depth for natural emitters and a negative-exponential distribution with depth for fallout radionuclides.

It is our customary practice to place the detector ~1 m above the soil surface. At this height, a tripod-mounted detector can be handled easily and still provide a radius of view for γ-emitting sources out to about 10 m. The source geometry for *in-situ* measurements can be considered as 2π or a "half-space;" however, soil and air attenuation effectively make it finite in size. An illustration of the relative contributions from the soil half-space of a medium energy (662 keV), aged-fallout ^{137}Cs-γ source is shown in Fig. 1. The "field of view" actually varies, being somewhat larger for higher energy sources and also for sources that are closer to the soil surface. Depending upon source energy, the detector effectively sees down to a depth of 15–30 cm.

Some investigators have used a collimator to limit the field of view of a detector (Cutshall and Larsen 1986), allowing for a simpler calibration procedure. Indeed, one may wish to measure small sections of ground under certain circumstances. However, for most applications, a more sensitive and representative measurement can be made by using a bare detector so that the full half-space is seen. One of the principal advantages of field spectrometry is that it averages out small-scale inhomogeneities of the source geometry that invariably are present. The amount of ground area viewed can be adjusted by simply varying the height of the detector. Although the results of the work described here are for a reference height of 1 m, they could be applied to any height between 0.5 and 2 m without any significant loss in accuracy.

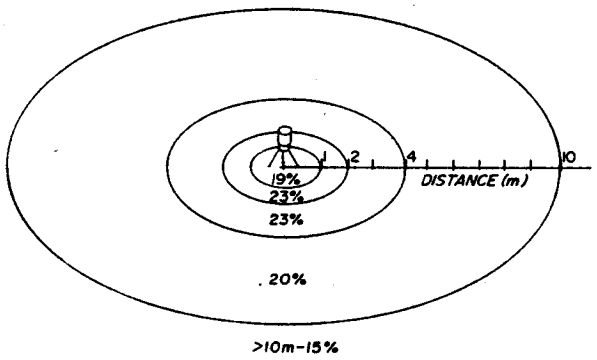


Fig. 1. Pictorial ground area representation of the relative contributions to the total 662 keV primary flux at 1 m above the ground for a ^{137}Cs source distribution where the depth parameter $\alpha/\rho = 0.21$ cm^2 g^{-1}.

CALIBRATION FOR FIELD SPECTROMETRY

A field calibration differs from that for laboratory sample counting in that spiked samples are not used. Rather a combination of experimental and theoretical methods are applied. We present here a summary of the procedure, and a complete description can be found in Beck et al. (1972).

The basic calibration equation for *in-situ* spectrometry can be expressed in terms of peak count rate (N), activity or inventory in the soil (A) and uncollided flux (ϕ) as

$$N_f/A = (N_f/N_0)(N_0/\phi)(\phi/A), \quad (1)$$

where the fundamental calibration parameters are expressed in ratios as follows:

N_f/A is the total-absorption peak count rate (cpm) in the spectrum at the energy of a particular nuclide γ transition per unit inventory (Bq m^{-2}) or concentration (Bq g^{-1}) of that nuclide in the soil,

N_f/N_0 is the angular correction factor of the detector at that energy for a given source distribution in the soil,

N_0/ϕ is the peak count rate (cpm) per unit uncollided flux (γ cm^{-2} s^{-1}) for a parallel beam of γ rays of the same energy that is incident-normal to the detector face, and

ϕ/A is the total uncollided flux (γ cm^{-2} s^{-1}) at that energy arriving at the detector per unit inventory or concentration of the nuclide in the soil.

In order to obtain the calibration factor (N_f/A) for a particular nuclide, the three quantities (N_f/N_0, N_0/ϕ and ϕ/A) are determined separately. The first two terms are detector dependent and can be determined experimentally, while the latter can be calculated on a purely theoretical basis. We will discuss these terms in some detail.

N_0/ϕ

The value of N_0/ϕ at a particular energy is obtained by counting a γ-emitting point source of known strength, placed at a distance of at least 1 m from the detector face, to simulate a parallel beam of normally incident radiation. The observed total-absorption peak count rate then is divided by the flux as computed from the inverse square law, corrected for air and source holder attenuation. Values of N_0/ϕ are determined in this manner at several different energies, and the results are plotted as a function of energy on log-log paper. Between 200 keV and 3 MeV, the data are fit to a straight line reasonably well. For any energy in this range, we can use the equation

$$\ln(N_0/\phi) = a - b \ln E, \quad (2)$$

where E is the energy of the γ line of interest (MeV), and a and b are constants which are detector dependent.

N_f/N_0

The angular correction factor (N_f/N_0) is dependent upon both the detector and source geometry. It is necessary to measure this factor because a cylindrical Ge detector generally does not have an isotropic response to γ rays incident at various zenith angles. Since the angular distribution of photons incident at the detector in the field varies with the source energy and distribution in the soil, N_f/N_0 is not a constant. However, as we will show later, the values generally do not vary by a large amount for a given detector. The value of N_f/N_0 for a particular energy and source distribution is calculated from

Table 1. ϕ – Unscattered flux (γ cm^{-2} s^{-1}) at 1 m above ground per unit source strength in the soil.*

Source energy (keV)	(α/ρ) – cm^2 g^{-1}					
	0 (Uniform)	0.0625	0.206	0.312	0.625	6.25	∞ (plane)
50	1.4403	0.0816	0.2245	0.3049	0.4748	1.147	1.577
100	2.7744	0.1458	0.3627	0.4708	0.6786	1.359	1.710
150	3.3264	0.1702	0.4103	0.5261	0.7438	1.427	1.775
200	3.9056	0.1843	0.4550	0.5770	0.8018	1.483	1.804
250	4.0640	0.2008	0.4697	0.5910	0.8185	1.506	1.863
364	4.7184	0.2268	0.5158	0.6429	0.8775	1.578	1.933
500	5.3904	0.2519	0.5595	0.6918	0.9334	1.650	1.995
662	6.1456	0.2788	0.6041	0.7412	0.9889	1.719	2.054
750	6.5312	0.2919	0.6257	0.7649	1.015	1.752	2.084
1000	7.5280	0.3245	0.6769	0.8209	1.077	1.830	2.151
1173	8.1472	0.3437	0.7067	0.8531	1.113	1.874	2.189
1250	8.4384	0.3523	0.7198	0.8675	1.129	1.895	2.205
1333	8.7504	0.3617	0.7336	0.8826	1.145	1.914	2.224
1460	9.1472	0.3731	0.7511	0.9011	1.166	1.941	2.247
1765	10.091	0.3997	0.7897	0.9428	1.211	1.997	2.294
2004	10.818	0.4188	0.8173	0.9725	1.243	2.036	2.334
2250	11.397	0.4357	0.8414	0.9982	1.271	2.071	2.358
2500	12.173	0.4536	0.8667	1.025	1.300	2.105	2.385

* For $\alpha/\rho = 0$ (uniform profile, natural emitters), the source strength is 1 γ g^{-1} s^{-1} for soil at all depths. For $\alpha/\rho > 0$ (exponential profile, fallout emitter), the source strength is 1 γ cm^{-2} s^{-1} emitted from an infinite column of soil where the activity exponentially decreases with depth at relaxation length of $1/\alpha$ at soil density ρ.

Table 2. Ge detector specifications.

Manufacturer	Serial No.	Code	Type	Cryostat orientation	Efficiency, (%)	Resolution at 1332 (keV)	Dimensions DxL (mm)	L/D+	Peak/Compton
Princeton* Gamma-tech	484	P1	Ge(Li)	4 L downward	2.9	1.70	38 X 20	0.56	23.0
	514	P2	Ge(Li)	4 L downward	12.2	2.43	43 X 44	1.02	30.0
	1039	P3	Ge(Li)	17 L upward	27.9	2.38	59 X 47	0.80	35.9
	1545	P4	Ge(Li)	17 L upward	22.3	2.10	58 X 54	0.96	49.5
	1030	P5	P-type Ge	2 L all attitude	21.7	1.77	59 X 35	0.59	52.0
EG&G Ortec**	23-N-37VB	01	N-type Ge	30 L upward	35.3	1.96	55 X 65	1.18	59.4
	25-N-1514	02	N-type Ge	30 L upward	35.4	1.73	55 X 72	1.31	67.9
	26-P-70P	03	P-type Ge	1.8 L all attitude	45.0	1.80	60 X 79	1.31	73.0

* Princeton Gamma-Tech, Inc., 1200 State Road, Princeton, NJ 08540

** EG & G Ortec, 100 Midland Road, Oak Ridge, TN 37830

\+ Ge crystal length/diameter ratio.

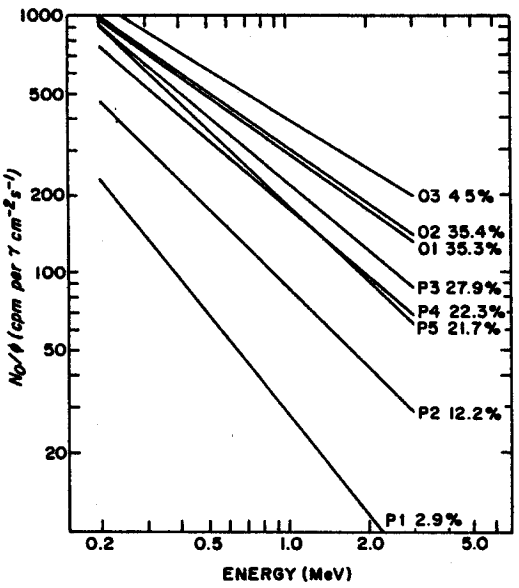


Fig. 2. Efficiency curves for parallel beam of radiation normal to the detector face (N_0/ϕ) for the various Ge detectors as listed by code number and quoted efficiency (ϵ).

$$N_f/N_0 = \frac{\int R(\theta)\phi(\theta)\mathrm{d}\theta}{\int \phi(\theta)\mathrm{d}\theta}, \qquad (3)$$

where $R(\theta)$ is the peak count rate for γ rays of energy E at angle θ, relative to the peak count rate at $\theta = 0°$ (normal incidence) and $\phi(\theta)$ is the γ-ray flux at energy E at angle θ.

In order to obtain the values of $R(\theta)$, the peak count rates are measured for point sources of various energies positioned at different angles at a fixed distance of at least 1 m to the detector. It is sufficient to perform this measurement at 15° intervals and draw a smooth curve through the experimental data. To obtain N_f/N_0, a numerical integration can be performed by using values of $\phi(\theta)$ that previously have been tabulated for various energies and source distributions (Beck et al. 1972).

In using the function $R(\theta)$ in the calculation of N_f/N_0, the direction the detector will face when in use must be taken into account. In general, the back end of a detector will have a low response to flux due to the attenuation effects of the cryostat. Consequently, the ideal orientation for a field detector is facing downward. This generally is accomplished by mounting on a tripod with the dewar overhead. In this position, the uncollided γ rays from the soil below will be incident between 0° and 90°, where 0° is defined as normal to the detector face. However, if a standard upward-facing cryostat is used, the range of angles from a ground source would be 180°–90° as measured from the normal to the detector face. Although a 30-L dewar might be thought of as shadowing the Ge crystal in this position, the amount of flux from the ground area being blocked is small compared to the total incident at the detector. For either the upward- or downward-facing case, it usually can be assumed that the detector has a symmetrical response about the azimuth because of its cylindrical shape. The results of our analysis for angular corrections presented in this paper cannot be applied to detectors that are oriented with their axis of symmetry parallel to the ground plane, such as would be the case for "goose-neck" cryostats.

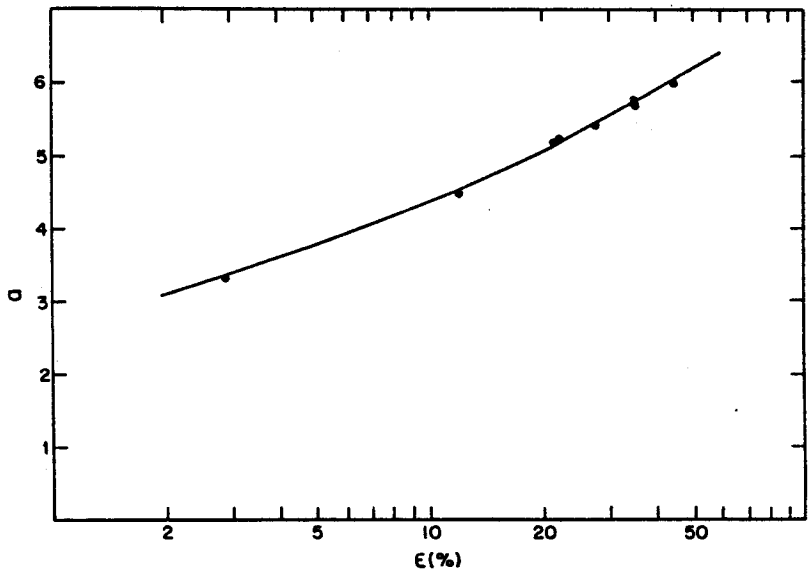


Fig. 3. Experimental values of the constant "a" as a function of detector efficiency (ϵ) and a quadratic fit to the data.

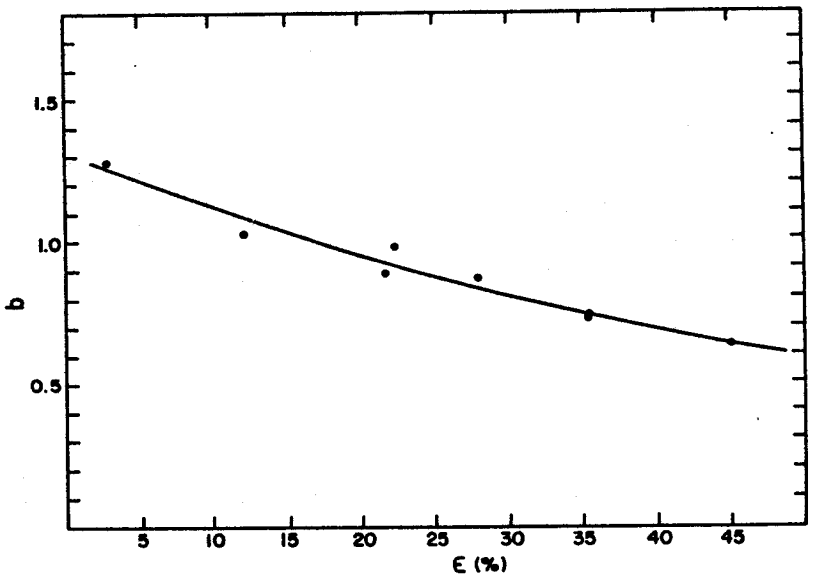


Fig. 4. Experimental values of the constant "b" as a function of detector efficiency (ϵ) and a quadratic fit to the data.

ϕ/A

The incident flux per unit inventory or concentration of the nuclide in the soil is not detector dependent, but rather a function of soil density and composition, air attenuation and the source distribution in the soil. Values of ϕ/A for various natural and man-made γ emitters found in the environment have been reported previously for uniform and exponential source-depth profiles in a representative soil mix (Beck et al. 1972). Values of the flux at various energies per unit-γ emission in the soil, reproduced from Beck et al. (1972), are given in Table 1. The parameter α/ρ in this table is a measure of the exponential profile, where α is the inverse of the relaxation length and ρ is the soil density. Thus, to compute a flux value for

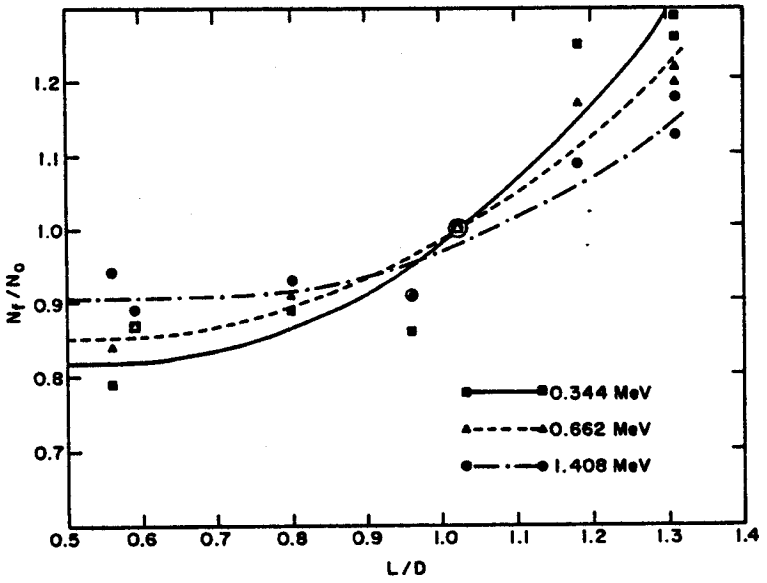


Fig. 5. Experimental angular correction factors (N_f/N_0) and fits as a function of the crystal length/diameter ratio at three different energies for a downward facing cyrostat for depth distribution of $\alpha/\rho = 0$ (uniform source distribution).

Table 3. Angular correction factor (N_f/N_0).*

Energy (Mev)	L/D 0.5	0.6	0.7	0.8	0.9	1.0	1.1	1.2	1.3
0.3	0.64	0.64	0.65	0.68	0.73	0.80	0.89	1.02	1.17
0.5	0.69	0.69	0.69	0.71	0.75	0.81	0.89	1.00	1.13
0.7	0.72	0.72	0.72	0.73	0.77	0.82	0.89	0.99	1.11
1.0	0.75	0.75	0.75	0.76	0.78	0.83	0.89	0.98	1.08
1.5	0.78	0.78	0.78	0.79	0.81	0.84	0.89	0.96	1.05
2.0	0.80	0.80	0.81	0.82	0.82	0.85	0.89	0.95	1.02
2.5	0.82	0.82	0.83	0.83	0.84	0.86	0.89	0.94	1.01

* Upward facing detector, uniform source distribution ($\alpha/\rho = 0$).

any arbitrary nuclide with a given depth distribution, a value of ϕ can be interpolated from Table 1 at a particular energy and then multiplied by the yield for that γ ray.

CALIBRATION RESULTS

The specifications of the eight detectors we calibrated using the above methods are listed in Table 2. As will be shown later, the crucial parameters for estimating detector calibration factors are the efficiency, orientation and crystal length/diameter ratio.

Figure 2 shows N_0/ϕ plotted as a function of energy for all eight detectors. As can be seen, these efficiency curves are nearly parallel. Thus, it would appear that they could be related in some way. Since it has become an industry standard to measure the efficiency of a Ge detector at 1332 keV relative to a 7.6 × 7.6 cm (3 × 3 in.) NaI(Tl) detector, we chose to use the manufacturer's quoted efficiency, which we denote as ϵ, to predict the response at other energies. The separate values of a and b (from eqn 2) for each detector are plotted as a function of ϵ in Figs. 3 and 4, respectively. A fit to a second degree polynomial in each case yielded:

$$a' = 2.689 + 0.4996 \ln \epsilon + 0.0969(\ln \epsilon)^2 \quad \text{and} \quad (4)$$

$$b' = 1.315 - 0.02044\epsilon + 0.00012\epsilon^2, \quad (5)$$

where the prime denotes the corresponding theoretical values of a and b. As can be seen, the fits are quite good. The maximum deviation from the curve fit for a is 2%, while that for b is 6%. These expressions for a' and b', therefore, can be used in eqn (2) to estimate the value of N_0/ϕ for any detector at any energy.

On a purely theoretical basis, the angular response of a detector should be related to the crystal dimensions. At low energies (<100 keV), the response will vary according to the surface area of the detector seen by the incident flux. At higher energies, a more complex three-dimensional analysis would be required. In addition, housing, mounting and dead-layer (inactive Ge) attenuation effects are present. Despite these complexities, we have found that the values of N_f/N_0 fit a relatively smooth curve when plotted as a function of the crystal length/diameter (L/D) ratio (e.g., see Fig. 5). Using this and similar figures, we have estimated N_f/N_0 values at various energies for both upward and downward facing detectors for the two most extreme cases of source depth distribution, uniform ($\alpha/\rho = 0$) and infinite plane ($\alpha/\rho = \infty$). The data set cover a range in crystal L/D values of 0.5–1.3 and are listed in Tables 3–6. Considering the relatively small variation of N_f/N_0 with the depth distribution, it is sufficient to apply the values for an infinite plane for any source near the soil surface. Cases of deeply distributed

Table 4. Angular correction factor (N_f/N_0).*

Energy (Mev)	L/D 0.5	0.6	0.7	0.8	0.9	1.0	1.1	1.2	1.3
0.3	0.77	0.77	0.78	0.78	0.81	0.89	1.00	1.12	1.34
0.5	0.79	0.79	0.80	0.80	0.83	0.90	0.99	1.10	1.28
0.7	0.80	0.80	0.81	0.82	0.84	0.90	0.99	1.09	1.24
1.0	0.82	0.82	0.82	0.83	0.86	0.91	0.98	1.08	1.20
1.5	0.83	0.83	0.83	0.85	0.87	0.92	0.98	1.06	1.16
2.0	0.84	0.84	0.84	0.86	0.88	0.92	0.98	1.05	1.13
2.5	0.85	0.85	0.85	0.87	0.89	0.92	0.97	1.05	1.10

* Upward facing detector, plane source distribution ($\alpha/\rho = \infty$).

Table 5. Angular correction factor (N_f/N_0).*

Energy (Mev)	L/D 0.5	0.6	0.7	0.8	0.9	1.0	1.1	1.2	1.3
0.3	0.81	0.82	0.83	0.86	0.91	0.99	1.08	1.18	1.31
0.5	0.84	0.85	0.85	0.88	0.93	0.99	1.06	1.14	1.25
0.7	0.86	0.86	0.87	0.90	0.93	0.98	1.05	1.12	1.21
1.0	0.88	0.88	0.89	0.91	0.94	0.98	1.03	1.10	1.18
1.5	0.91	0.91	0.91	0.92	0.94	0.97	1.02	1.07	1.13
2.0	0.92	0.92	0.93	0.93	0.94	0.96	1.00	1.05	1.10
2.5	0.94	0.94	0.94	0.94	0.95	0.96	0.99	1.03	1.07

* Downward facing detector, uniform source distribution ($\alpha/\rho = 0$).

Table 6. Angular correction factor (N_f/N_0).*

Energy (Mev)	L/D 0.5	0.6	0.7	0.8	0.9	1.0	1.1	1.2	1.3
0.3	0.80	0.80	0.81	0.83	0.88	0.97	1.07	1.19	1.35
0.5	0.82	0.82	0.83	0.85	0.90	0.97	1.06	1.16	1.29
0.7	0.83	0.84	0.85	0.87	0.91	0.97	1.05	1.14	1.25
1.0	0.85	0.85	0.86	0.88	0.92	0.97	1.04	1.12	1.22
1.5	0.86	0.87	0.88	0.90	0.93	0.97	1.03	1.10	1.17
2.0	0.88	0.89	0.90	0.91	0.93	0.97	1.02	1.08	1.14
2.5	0.89	0.90	0.91	0.92	0.94	0.97	1.01	1.07	1.12

* Downward facing detector, plane source distribution ($\alpha/\rho = \infty$).

sources ($\alpha/\rho < 0.1$) should have the values for a uniform profile applied, while a median value of N_f/N_0 can be applied to somewhat aged fallout products that have not penetrated far into the soil ($0.1 < \alpha/\rho < 0.5$).

ESTIMATED CALIBRATION FACTORS

The conversion of an observed peak count rate to a radionuclide inventory or concentration in the soil can be performed by determining the three separate factors N_0/ϕ, N_f/N_0 and ϕ/A and using eqn (1). This procedure is outlined in example 2 in the appendix. To save most of the steps of this operation, we have taken the results of our fit of N_0/ϕ to ϵ and combined them with the values of ϕ as derived from Table 1 to yield the factor N_0/A for some common natural and man-made radionuclides. These values are presented in Tables 7–9 for detectors with efficiencies ranging between 5–45% in steps of 5%. The values for any arbitrary detector in this range can be interpolated from this listing. These N_0/A values represent the peak count rates to inventory or concentration conversion factor for a detector where $N_f/N_0 = 1$, that is, where there is no angular correction factor. Also listed in these tables are the factors to convert the inventory or concentration to exposure rate and dose rate in air at a height of 1 m above the ground.

In Table 7, the factors for man-made emitters were calculated using an exponential depth distribution where $\alpha/\rho = 6.25$, which corresponds to a source that has penetrated somewhat into the soil. At a typical soil density of 1.6 g cm^{-3}, this would mean that 63% ($1 - 1/e$) of the activity was contained in the top 1 mm of soil. We have found from past experiences that this represents a reasonable approximation to a fresh deposition of fallout. Aside from some penetration of a fallout product below the soil surface, this type of profile can result from the effects of ground roughness, which, in effect, makes a surface source appear deeper to the detector.

Table 8 contains factors for the ubiquitous ^{137}Cs for various depth profiles. We include this information for this nuclide, because it contributes several percent to the total γ-exposure rate in most areas, and, in a sense, can be considered part of the "background" radiation environment. As a weapons test fallout product that was deposited for the most part in the late 1950s and early 1960s, this nuclide has assumed a depth profile in undisturbed soils that varies among sites throughout the U.S. In general, one can expect the current profile to be reasonably well represented by an exponential function, where α/ρ is on the order of .03–.2 for open field areas where the climate is moist and from .2–1 for semi-arid areas.

The listing in Table 9 is for natural emitters assuming a uniform source distribution. As such, the quantity in-

Table 7. N_0/A^* for freshly deposited man-made emitters (α/ρ = 6.25).

Nuclide	Energy (MeV)	Dose rate (exposure rate)**	Detector efficiency (%) 5	10	15	20	25	30	35	40	45
^{60}Co	1.173	8.94×10^{-3} (3.77×10^{-2})	0.0065 (0.24)	0.0122 (0.45)	0.0184 (0.68)	0.0251 (0.93)	0.0327 (1.21)	0.041 (1.50)	0.049 (1.82)	0.058 (2.16)	0.068 (2.51)
	1.332		0.0057 (0.21)	0.0108 (0.40)	0.0165 (0.61)	0.0230 (0.85)	0.0297 (1.10)	0.038 (1.39)	0.046 (1.69)	0.055 (2.02)	0.064 (2.37)
^{95}Zr	.724	2.84×10^{-3} (1.20×10^{-2})	0.0046 (0.17)	0.0084 (0.31)	0.0122 (0.45)	0.0159 (0.59)	0.0200 (0.74)	0.0241 (0.89)	0.0281 (1.04)	0.032 (1.20)	0.037 (1.37)
	.757		0.0057 (0.21)	0.0103 (0.38)	0.0149 (0.55)	0.0195 (0.72)	0.0243 (0.90)	0.0295 (1.09)	0.035 (1.29)	0.040 (1.49)	0.046 (1.69)
^{95}Nb	.768	2.94×10^{-3} (1.24×10^{-2})	0.0103 (0.38)	0.0184 (0.68)	0.0268 (0.99)	0.035 (1.31)	0.044 (1.64)	0.054 (1.98)	0.063 (2.34)	0.073 (2.70)	0.083 (3.08)
^{103}Ru	.497	1.86×10^{-3} (7.85×10^{-3})	0.0141 (0.52)	0.0243 (0.90)	0.034 (1.26)	0.044 (1.61)	0.053 (1.95)	0.062 (2.29)	0.071 (2.63)	0.080 (2.97)	0.090 (3.31)
^{131}I	.365	1.50×10^{-3} (6.32×10^{-3})	0.0184 (0.68)	0.031 (1.14)	0.042 (1.56)	0.053 (1.95)	0.062 (2.31)	0.072 (2.65)	0.081 (2.98)	0.089 (3.30)	0.098 (3.62)
^{132}I	.668+.670	8.67×10^{-3} (3.66×10^{-2})	0.0122 (0.45)	0.0216 (0.80)	0.031 (1.16)	0.041 (1.52)	0.051 (1.88)	0.061 (2.25)	0.071 (2.63)	0.082 (3.02)	0.092 (3.42)
	.773		0.0078 (0.29)	0.0141 (0.52)	0.0203 (0.75)	0.0270 (1.00)	0.034 (1.25)	0.041 (1.51)	0.048 (1.78)	0.056 (2.06)	0.064 (2.35)
^{134}Cs	.605	6.02×10^{-3} (2.54×10^{-2})	0.0130 (0.48)	0.0227 (0.84)	0.0322 (1.19)	0.042 (1.55)	0.052 (1.91)	0.061 (2.27)	0.071 (2.63)	0.081 (3.00)	0.091 (3.38)
	.796		0.0084 (0.31)	0.0151 (0.56)	0.0222 (0.82)	0.0295 (1.09)	0.037 (1.37)	0.045 (1.66)	0.053 (1.96)	0.061 (2.27)	0.070 (2.60)
^{136}Cs	.819	8.11×10^{-3} (3.42×10^{-2})	0.0095 (0.35)	0.0173 (0.64)	0.0251 (0.93)	0.034 (1.24)	0.042 (1.57)	0.051 (1.90)	0.061 (2.25)	0.071 (2.61)	0.081 (2.99)
	1.048		0.0059 (0.22)	0.0108 (0.40)	0.0162 (0.60)	0.0219 (0.81)	0.0284 (1.05)	0.035 (1.29)	0.042 (1.55)	0.050 (1.83)	0.057 (2.12)
^{137}Cs	.662	2.20×10^{-3} (9.28×10^{-3})	0.0103 (0.38)	0.0181 (0.67)	0.0259 (0.96)	0.034 (1.26)	0.042 (1.56)	0.051 (1.87)	0.059 (2.18)	0.068 (2.50)	0.077 (2.83)
^{140}Ba	.537	5.71×10^{-4} (2.41×10^{-3})	0.0038 (0.14)	0.0062 (0.23)	0.0089 (0.33)	0.0116 (0.43)	0.0141 (0.52)	0.0165 (0.61)	0.0192 (0.71)	0.0216 (0.80)	0.0243 (0.90)
^{140}La	.487	7.89×10^{-3} (3.33×10^{-2})	0.0078 (0.29)	0.0135 (0.50)	0.0189 (0.70)	0.0241 (0.89)	0.0292 (1.08)	0.034 (1.26)	0.039 (1.44)	0.044 (1.63)	0.049 (1.81)
	1.596		0.0046 (0.17)	0.0086 (0.32)	0.0135 (0.50)	0.0189 (0.70)	0.0254 (0.94)	0.032 (1.18)	0.039 (1.45)	0.047 (1.75)	0.056 (2.07)

* cpm per Bq m^{-2}
(cpm per mCi km^{-2})

** Dose rate in air (exposure rate) conversion factors for above:
nGy h^{-1} per Bq m^{-2} (μR h^{-1} per mCi km^{-2})

Table 8. N_0/A^* for ^{137}Cs (.662 MeV) at various depth profiles.

a/ρ	Dose rate in air (exposure rate)**	Detector efficiency (%)								
		5	10	15	20	25	30	35	40	45
∞	2.53×10^{-3} (1.07×10^{-2})	0.0121 (0.447)	0.0214 (0.790)	0.031 (1.14)	0.040 (1.49)	0.050 (1.85)	0.060 (2.21)	0.070 (2.58)	0.080 (2.96)	0.090 (3.34)
6.250	2.20×10^{-3} (9.30×10^{-3})	0.0102 (0.378)	0.0181 (0.669)	0.0260 (0.963)	0.034 (1.26)	0.042 (1.56)	0.050 (1.87)	0.059 (2.18)	0.068 (2.50)	0.076 (2.83)
0.625	1.47×10^{-3} (6.21×10^{-3})	0.0059 (0.218)	0.0097 (0.385)	0.0150 (0.554)	0.0196 (0.725)	0.0243 (0.899)	0.0292 (1.08)	0.034 (1.26)	0.039 (1.44)	0.044 (1.63)
0.312	1.19×10^{-3} (5.02×10^{-3})	0.0044 (0.163)	0.0078 (0.289)	0.0112 (0.416)	0.0147 (0.544)	0.0182 (0.674)	0.0218 (0.807)	0.0255 (0.942)	0.0292 (1.08)	0.033 (1.22)
0.206	1.02×10^{-3} (4.32×10^{-3})	0.0038 (0.133)	0.0064 (0.235)	0.0091 (0.337)	0.0119 (0.442)	0.0148 (0.548)	0.0177 (0.655)	0.0207 (0.765)	0.0237 (0.877)	0.0268 (0.992)
0.0625	5.52×10^{-4} (2.33×10^{-3})	0.0016 (0.061)	0.0029 (0.109)	0.0042 (0.156)	0.0055 (0.205)	0.0069 (0.254)	0.0082 (0.304)	0.0096 (0.354)	0.0110 (0.406)	0.0124 (0.460)

* cpm per Bq m^{-2}
(cpm per mCi km^{-2})

** Dose rate in air (exposure rate) conversion factors for above:
nGy h^{-1} per Bq m^{-2} (μR h^{-1} per mCi km^{-2})

Table 9. N_0/A^* for uniform distribution of natural emitters ($\alpha/\rho = 0$).

Nuclide	Energy (MeV)	Detector efficiency (%)								
		5	10	15	20	25	30	35	40	45
					Uranium series					
^{226}Ra	.186	0.042 (1.57)	0.067 (2.46)	0.086 (3.17)	0.101 (3.74)	0.114 (4.21)	0.125 (4.62)	0.135 (4.98)	0.144 (5.31)	0.152 (5.63)
^{214}Pb	.242	0.070 (2.59)	0.113 (4.17)	0.148 (5.49)	0.179 (6.62)	0.206 (7.61)	0.230 (8.49)	0.251 (9.30)	0.273 (10.1)	0.292 (10.8)
	.295	0.154 (5.70)	0.252 (9.33)	0.338 (12.5)	0.414 (15.3)	0.484 (17.9)	0.546 (20.2)	0.608 (22.5)	0.665 (24.8)	0.722 (26.7)
	.352	0.256 (9.46)	0.427 (15.8)	0.581 (21.5)	0.722 (26.7)	0.854 (31.6)	0.978 (36.2)	1.10 (40.6)	1.21 (44.9)	1.33 (49.2)
^{214}Bi	.609	0.206 (7.62)	0.362 (13.4)	0.516 (19.1)	0.670 (24.8)	0.827 (30.6)	0.984 (36.4)	1.14 (42.3)	1.30 (48.2)	1.47 (54.3)
	1.120	0.044 (1.62)	0.082 (3.02)	0.123 (4.55)	0.168 (6.21)	0.217 (8.01)	0.269 (9.94)	0.324 (12.0)	0.384 (14.2)	0.446 (16.5)
	1.765	0.033 (1.22)	0.064 (2.36)	0.100 (3.70)	0.142 (5.25)	0.189 (7.00)	0.242 (8.96)	0.300 (11.1)	0.365 (13.5)	0.435 (16.1)
					Thorium series					
^{228}Ac	.911	0.097 (3.57)	0.176 (6.52)	0.261 (9.64)	0.349 (12.9)	0.443 (16.4)	0.543 (20.1)	0.649 (24.0)	0.757 (28.0)	0.870 (32.2)
	.965+.967	0.073 (2.70)	0.134 (4.95)	0.199 (7.36)	0.268 (9.93)	0.343 (12.7)	0.422 (15.6)	0.503 (18.6)	0.589 (21.8)	0.678 (25.1)
$^{212}Pb+^{224}Ra$	.239+.241	0.470 (17.4)	0.757 (28.0)	0.995 (36.8)	1.200 (44.4)	1.38 (51.0)	1.54 (56.9)	1.68 (62.3)	1.82 (67.4)	1.96 (72.4)
^{208}Tl	.583	0.141 (5.21)	0.246 (9.10)	0.351 (13.0)	0.454 (16.8)	0.557 (20.6)	0.660 (24.4)	0.765 (28.3)	0.870 (32.2)	0.978 (36.2)
	2.615	0.059 (2.19)	0.119 (4.41)	0.193 (7.15)	0.283 (10.5)	0.389 (14.4)	0.511 (18.9)	0.651 (24.1)	0.808 (29.9)	0.981 (36.3)
^{40}K	1.461	0.026 (0.97)	0.050 (1.84)	0.077 (2.84)	0.107 (3.97)	0.141 (5.22)	0.178 (6.60)	0.219 (8.09)	0.262 (9.71)	0.308 (11.4)

* cpm per Bq kg^{-1}
(cpm per pCi g^{-1})

Note: Dose rate in air (exposure rate) conversion factors for above:

^{238}U series 0.450 nGy h^{-1} per Bq kg^{-1} (1.90 μR h^{-1} per pCi g^{-1})

^{232}Th series 0.668 nGy h^{-1} per Bq kg^{-1} (2.82 μR h^{-1} per pCi g^{-1})

^{40}K 0.0424 nGy h^{-1} per Bq kg^{-1} (0.179 μR h^{-1} per pCi g^{-1})

ferred is in the form of a concentration, independent of depth and soil density. In most cases, there is equilibrium among the various nuclides in the U and Th series, so that the measurement of any one line yields a concentration value for the entire series, although averaging several lines will give a more precise value. Exhalation of ^{222}Rn from the soil complicates the task of evaluating the U series; however, this effect tends to produce only a 10–20% reduction in the important γ-emitting ^{214}Pb and ^{214}Bi daughter products in the surface soil, which is offset somewhat by the contribution of the flux from these same nuclides in the ambient air. A detailed evaluation of this phenomena can be found in Beck (1974). The ϕ/A values used to compute the ^{226}Ra and progeny in this table are based on an intensity of 0.45 per disintegration for the .609 MeV ^{214}Bi line, which differs from the intensity of 0.43 reported in Beck et al. (1972).

Before applying the N_0/A values from these tables to the peak count rates in a field spectrum, it is necessary to multiply by the appropriate angular correction factor (N_f/N_0) from Tables 3–6 in order to obtain N_f/A.

DISCUSSION OF ERRORS AND LIMITATIONS

Although the results obtained by applying the semi-empirical calibration data provided here cannot be expected to be as accurate as those based on an actual experimental calibration, we believe that they would fall within reasonable error bounds. As a measure of the expected accuracy, the estimated conversion factors as computed by the above method for the eight detectors used in this study were compared to the experimental values. For energies above 500 keV, the differences were generally <5% with no value exceeding 7%. Since this comparison can be made only for the present limited set of eight detectors, we conservatively estimate that the uncertainty in our estimated calibration factors is on the order of 10%. Somewhat larger differences between the estimated and experimental values were found for energies between 200 and 500 keV, so we conservatively estimated the uncertainty in this energy range to be 15%. Considering the convenience of being able to apply this semi-empirical calibration without performing any laborious experimental work and associated calculations, this degree of accuracy seems reasonably acceptable.

In addition to any systematic errors that may be introduced in applying the calibration described here, there are the usual statistical counting errors associated with the analysis of spectrum peaks. These counting errors are related to the level of activity present at a site and the detector efficiency and counting time. For an average size detector of 25% efficiency and a counting time of one h, the results for typical levels of natural background emitters would have a coefficient of variation of 5% or less. The lower limit of detection for common fission products such as those listed in Table 8 using a detector of this size would be on the order of a 100 Bq m^{-2} for only a 10-min count.

A good check to perform when making field measurements is to sum the individual exposure rates for each radionuclide (natural and man-made) and, after adding in the cosmic-ray contribution to the total air ionization, compare the result to a reading obtained from a pressurized ionization chamber. When the two values are in agreement, one can assume the Ge detector calibration being used is correct. In cases where there is some uncertainty in the history of the site, this comparison also serves to insure that the assumed source distributions are correct as well. To make this comparison, we present for the reader's convenience in Fig. 6 the cosmic-ray secondary-exposure-rate equivalent and dose rate in air as a function of altitude and barometric pressure for mid-latitudes as derived from Lowder and Beck (1966). In a strict sense, the quantity "exposure rate" is only applied to γ rays of certain energies. However, for environmental radiation measurements, it is convenient to extend the meaning to include the exposure-rate equivalent of ionization due to cosmic rays. These values vary with the 11-y solar cycle being a few percent higher at solar minimum and lower at solar maximum (O'Brien 1972).

The conversion factors presented in Table 7 are somewhat sensitive to the depth profile of the nuclide in the soil. We have chosen a source distribution, where $\alpha/\rho = 6.25$, because it is applicable to the case of a fresh deposit that would occur if there were releases to the environment from an accident at a nuclear facility. For sources that are distributed more deeply in the soil, such as ^{137}Cs from global-weapons-tests fallout, the application of these factors would underestimate the inventory. However, the exposure rate that would be inferred from the data in Table 7 still would be reasonably close to the true value. This results because the observed peak count rate in a field spectrum is essentially a measure of the uncollided flux, and, although both the uncollided flux and the exposure rate for a given inventory vary significantly with the source depth distribution, the ratio of these two quantities does not vary significantly.

In cases where a deeper profile of the nuclide is suspected, one can take soil samples from different depths for laboratory analysis to determine the true profile (Miller and Helfer 1985). The correct conversion factor to apply in order to obtain an inventory estimate then can be calculated using the ϕ values from Table 1 to generate a table analogous to Table 9 for ^{137}Cs. For a comprehensive listing of the corresponding exposure-rate per unit inventory factor that must be applied in these cases, we refer the reader to Beck (1980).

CONCLUSIONS

In-situ γ-ray spectrometry is a practical tool for obtaining information on radionuclides in the environment. It is particularly useful in emergency-response situations where a rapid assessment of deposited activity and exposure rates for specific radionuclides is desired. It is also a sensitive method that can be used for routine checking

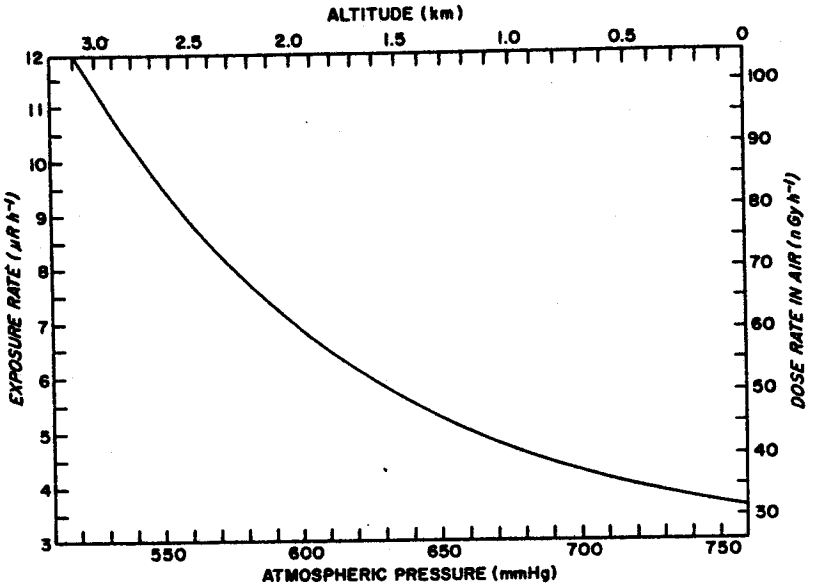


Fig. 6. Cosmic-ray-exposure rates and dose rates in air as a function of altitude and atmospheric pressure at mid-latitudes.

of low-level contamination in the environment. Since a complete calibration of a Ge detector for field measurements involves a considerable amount of effort, the calibration factors given in this paper can be used in situations where an approximation will suffice. The only parameters that are needed are the manufacturer's quoted efficiency at 1332 keV, the detector orientation (up or down) and the Ge crystal length/diameter ratio. Despite the variation in detector response that results from other variables such as crystal mounting, housing and dead layers, it would appear that the accuracy of using these semi-empirical calibration factors is on the order of 10–15%.

REFERENCES

Beck, H. L. Gamma radiation from radon daughters in the atmosphere. J. Geophys. Res. 79:2215–2221; 1974.

Beck, H. L. Exposure rate conversion factors for radionuclides deposited on the ground. New York: U.S. Department of Energy, Environmental Measurements Laboratory; EML-378; 1980.

Beck, H. L.; De Campo, J.; Gogolak, C. V. *In situ* Ge(Li) and Na(Tl) gamma-ray spectrometry. New York: U.S. Department of Energy, Environmental Measurements Laboratory; HASL-258; 1972.

Cutshall, N. H.; Larsen, I. L. Calibration of a portable intrinsic Ge γ-ray detector using point sources and testing for field applications. Health Phys. 51:53–59; 1986.

Gogolak, C. V. Rapid determination of noble gas radionuclide concentrations in power reactor plumes. Health Phys. 46: 783–792; 1984.

Gogolak, C. V.; Winkelmann, I.; Weimar, S.; Wolff, S.; Klopfer, P. Observations of Chernobyl fallout in Germany by *in situ* gamma-ray spectrometry. In: Volchok, H. L.; Chieco, N. A., eds. A compendium of the Environmental Measurements Laboratory's research projects related to the Chernobyl nuclear accident. New York: U.S. Department of Energy, Environmental Measurements Laboratory Publication; EML-460; 1986.

Lowder, W. M.; Beck, H. L. Cosmic ray ionization in the lower atmosphere. J. Geophys. Res. 71:4661–4667; 1966.

Miller, K. M.; Beck, H. L. Indoor gamma and cosmic ray exposure rate measurements using a Ge spectrometer and pressurized ionization chamber. Radiat. Protec. Dosim. 7:185–189; 1984.

Miller, K. M.; Gogolak, C. V.; Boyle, M.; Gulbin, J. Radiation measurements following the Three Mile Island reactor accident. New York: U.S. Department of Energy, Environmental Measurements Laboratory Publication; EML-357; 1979.

Miller, K. M.; Helfer, I. K. *In situ* measurements of ^{137}Cs inventory in natural terrain. In: Proceedings of the Health Physics Society midyear topical symposium; (6–10 January) 1985; Colorado Springs, CO: Central Rocky Mountain Chapter of the Health Physics Society; 1985:243–251.

O'Brien, K. The cosmic ray field at ground level. In: Proceedings of the second international symposium on the natural radiation environment; (7–11 August 1972); Houston, TX; New York: U.S. Energy Research and Development Administration: The Natural Radiation Environment II; Vol 1, 1972: 15–54.

APPENDIX

For clarity, we will provide two examples that show how to use the calibration method described in this paper.

Example 1

In this first example, we will use a hypothetical detector with a downward facing cryostat, 30% efficiency and a crystal length/diameter (L/D) ratio of 1.0. The nuclide we wish to measure is ^{131}I (.365 keV), a freshly deposited man-made emitter (Table 7).

(1) From Table 6, we estimate the angular correction factor N_f/N_0 for .365 keV and L/D ratio of 1.0. The N_f/N_0 value for this energy is seen to be 0.97.

(2) The N_0/A can be obtained by using Table 7. The value from Table 7 is 0.072.

(3) These two values are multiplied to compute N_f/A.

$$N_f/A = (0.072 \text{ cpm per Bq m}^{-2})(0.97)$$

or

$$N_f/A = 0.070 \text{ cpm per Bq m}^{-2}.$$

(4) If the measured peak count rate is at 100 cpm, then the activity deposited is:

$$A = 100 \text{ cpm}/0.070 \text{ cpm per Bq m}^{-2}$$

or

$$A = 1.43 \times 10^3 \text{ Bq m}^{-2}.$$

(5) Using the conversion factor from Table 7, the contribution to the dose rate would be:

$$I = (1.5 \times 10^{-3} \text{ nGy h}^{-1} \text{ per Bq m}^{-2})(1.43 \times 10^3 \text{ Bq m}^{-2})$$

or

$$I = 2.14 \text{ nGy h}^{-1}.$$

Example 2

In this example, we will compute N_f/A for an arbitrary nuclide with a given depth distribution by knowing the following information about the detector and the nuclide to be analyzed.

The detector will have the same characteristics as in example 1, but the nuclide will be Ag-110M at .658 MeV with a source distribution of $\alpha/\rho = 6.25$, which corresponds to a slightly buried source. We will compute N_f/A using the three terms in eqn (1).

(1) The angular correction factor (N_f/N_0) is interpolated from Table 6 to be 0.97.

(2) Using eqns (4) and (5), where ϵ is set equal to 30, we find the values for a' to be 5.509 and b' to be 0.810. Incorporating the values of a' and b' in eqn (2), we calculate N_0/ϕ to be 347.

(3) Using the data in Table 1, we interpolate and find the flux for unit γ emission to be 1.72, which is multiplied by the yield for that γ ray (γ per disintegration).

$$\phi/A = (1.72)(0.947)$$

$$\phi/A = 1.63\gamma \text{ cm}^{-2} \text{ s}^{-1} \text{ per Bq cm}^{-2}$$

or

$$\phi/A = 1.63 \times 10^{-4}\gamma \text{ cm}^{-2} \text{ s}^{-1} \text{ per Bq m}^{-2}.$$

(4) N_f/A is then

$$N_f/A = (0.97)(347)(1.63 \times 10^{-4})$$

or

$$N_f/A = 0.0549 \text{ cpm per Bq m}^{-2}.$$

(5) For a peak count rate of 100 cpm, then

$$A = 100 \text{ cpm}/0.0549 \text{ cpm per Bq m}^{-2}$$

or

$$A = 1.82 \times 10^3 \text{ Bq m}^{-2}.$$

(6) Using Beck (1980), the exposure rate for 1 mCi km^{-2} is given as .0436 μR h^{-1} for this source distribution, $\alpha/\rho = 6.25$. In SI dose units, this is equivalent to .0103 nGy h^{-1} per Bq m^{-2}.

$$I = (0.0103)(1.82 \times 10^3)$$

or

$$I = 18.8 \text{ nGy h}^{-1}.$$